Highly Sensitive Determination of Folic Acid Using Graphene Oxide Nanoribbon Film Modified Screen Printed Carbon Electrode

Veerappan Mani[1,2], Rajaji Umamaheswari[3], Shen-Ming Chen[1,], Mani Govindasamy[1], Chaochin Su[3], Anandaraj Sathiyan[4], Johnson Princy Merlin[4], Murugan Keerthi[5]*

[1] Department of Chemical Engineering and Biotechnology, National Taipei University of Technology, Taipei, Taiwan 106 (ROC)
[2] Graduate Institute of Biomedical and Biochemical Engineering, National Taipei University of Technology, Taipei, Taiwan (ROC)
[3] Institute of Organic and Polymeric Materials, National Taipei University of Technology, Taipei 10608, Taiwan
[4] Department of Chemistry, Bishop Heber College (Autonomous), Tiruchirappalli–620 017, Tamil Nadu, India
[5] Department of Analytical Chemistry, University of Madras, Guindy Campus, Chennai–600 025, Tamil Nadu, India
[*]E-mail: smchen78@ms15.hinet.net

A cost-effective screen printed electrode modified with graphene oxide nanoribbon (GONR) is developed for the determination of folic acid (FA). GONR is prepared from multi-walled carbon nanotubes (MWCNTs) and our studies revealing that the electrocatalytic ability of MWCNTs is greatly improved in GONR. The GONR is successfully characterized by SEM, EDX and impedance analysis. Next, GONR was deposited on the pretreated screen printed carbon electrode (SPCE) and the resulting GONR/SPCE was used to study the electrocatalysis of FA. The fabricated modified electrode has excellent electrocatalytic ability to detect FA. The effect of scan rate and pH towards electrocatalysis of FA is studied in detailed. The electrode detects FA in wide linear range of 0.1–1600 μM and achieves low detection limit of 20 nM. The sensor performance of the GONR/SPCE is either superior or comparable to the previously published FA sensors. Moreover, the electrode has good repeatability, reproducibility, stability and practicality.

1. INTRODUCTION

Folic acid (FA) is a B-group vitamin which has a major role in biological functions of cell metabolism like DNA replication, repair and methylation, synthesis of nucleotides, vitamins, amino acids etc. [1-3]. Its deficiency in our body leads to several disorders including increased risk of colorectal cancer, neural tube defects, hypomethylation and it potentially induces proto-oncogene expression leading to cancer [4-6]. FA is available as supplements and its sensitive determination is highly important in food and pharmaceutical samples [7-9]. Unmodified electrodes are poor in selectivity and sensitivity and hence several chemically modified electrodes are reported for FA detection [1, 10-13]. Recently, graphene based nanomaterials are popularly used in electrochemical sensing applications due to their peculiar physiochemical properties [8, 14-18]. More recently, graphene oxide nanoribbons (GONR), a derivative of multiwalled carbon nanotubes (MWNCTs) is emerging as excellent carbonaceous nanomaterial in diverse range of applications [19-21]. GONR can be easily prepared through unzipping of MWCNTs [22-25]. GONR has significantly higher rich edge chemistry and abundant functional groups than MWCNTs and hence GONR is expected to be better electrode modifiers than MWCNTs based modifiers in electrochemical sensors [26-28]. Herein, we are demonstrating the electrochemical sensing ability of GONR towards determination of FA and our studies revealed that GONR is better electrocatalytic material to FA in comparison with MWCNTs. GONR is prepared through acid treatment and its formation was confirmed through SEM, EDX and EIS analysis. We have adopted screen printed carbon electrodes (SPCE) to prepare working electrode because of its low-cost, easy fabrication, flexibility, and reproducibility [29, 30] .

2. EXPERIMENTAL

2.1 Chemicals and Apparatus

MWCNTs (bundled> 95%), FA and all other reagents including solvents were purchased from Sigma-Aldrich and used as received. Electrochemical studies were performed in a conventional three electrode cell using modified SPCE as a working electrode (area 0.3 cm^2), saturated Ag|AgCl (saturated KCl) as a reference electrode and Pt wire as a counter electrode. The SPCEs were purchased from Zensor R&D Co., Ltd., Taipei, Taiwan. The supporting electrolyte used for the electrochemical studies was 0.1 M phosphate buffer (pH 7) prepared from sodium dihydrogen phosphate and disodium hydrogen phosphate. 0.1 M acetate buffer (for pH 3 and 5), 0.1 M phosphate buffer (for pH 7) and 0.1 M Tris-buffered saline (for pH 9) were prepared and used for different pH studies.

All the electrochemical measurements were carried out using CHI 1205A electrochemical work station (CH Instruments, Inc., U.S.A). Scanning electron microscope (SEM) images were taken using Hitachi S-3000 H and Energy-dispersive X-ray (EDX) analysis were carried out using Horiba Emax x-act (Sensor + 24 V=16 W, resolution at 5.9 keV). The electrochemical impedance spectroscopy (EIS) studies were performed using EIM6ex Zahner (Kronach, Germany).

2.2 Preparation of graphene oxide nanoribbons

300 mg of MWCNTs were added to 80 mL H_2SO_4 and stirred for 1 h. Subsequently, 8 mL H_3PO_4 was added and the solution was stirred for another 20 min. Next, 2.5 g of $KMnO_4$ was added and the whole mixture was heated at 65°C for 2 h and finally cooled to room temperature. Afterwards, the reaction mixture was poured on 100 mL of ice containing 10 mL 30% H_2O_2. The obtained brown colored sediment was filtered and washed with 100 mL of water. Next, it was washed with 3× with HCl (20 vol%, 25 mL each), 2 × with ethanol (20 mL each) and 2 × with ether (20 mL each). Finally, the purified GONR is vacuum dried for overnight at 80°C and redispersed in water (0.5 mg mL^{-1}).

2.3 Preparation of modified SPCE

First, the SPCE was preanodized by applying 2.0 V (vs. Ag/AgCl) constant potential for 300 s in 0.1 M phosphate buffer (pH 7) [31, 32]. Then, 6 µl dispersions of GONRs are drop casted on the preanodized SPCE surface and dried at ambient conditions.

3. RESULTS AND DISCUSSION

3.1 Characterizations

The SEM images of GONRs (Fig. 1A and B) clearly reveal the ribbon-like morphology of GONR which is consistent with the previous reports [33-35]. The EDX spectrum of GONRs (Fig. 2A) confirmed the presences of expected elements, carbon (C) and oxygen (O) with weight% of 59.85 and 40.15, respectively. The electrochemical impedance spectroscopy studies are performed in order to examine the electrical and interfacial properties of the fabricated modified films on the electrode surface [36-38]. Figure 2B displays the EIS curves obtained at unmodified SPCE (a), GONR/SPCE (b) and MWCNTs/SPCE (c) in 0.1 M KCl containing 5 mM $Fe(CN)_6^{3-/4-}$. Randles equivalent circuit model has been used to fit the experimental data (inset to Figure 2B) and the corresponding data are represented as Nyquist plots [16, 39]. The EIS parameters such as, R_s, R_{ct} C_{dl} and Z_w are stands for electrolyte resistance, charge transfer resistance, double layer capacitance and Warburg impedance, respectively. Interestingly, the diameters of the semicircle portion for each EIS curves are different for different modifiers. The charge transfer resistance (R_{ct}) values obtained at SPCE, MWCNTs/SPCE and GONRs/SPCE are 185.6, 39.8, 79.54 Ω, respectively. The R_{ct} value obtained at GONRs/SPCE is larger than the MWCNTs/SPCE due to the high resistance of GONR compared with MWCNTs. The presence of oxygen functionalities on the surface of GONR leads to little drop in conductivity; however these oxygen functional groups enhance the electrocatalytic ability of the material [26, 40].
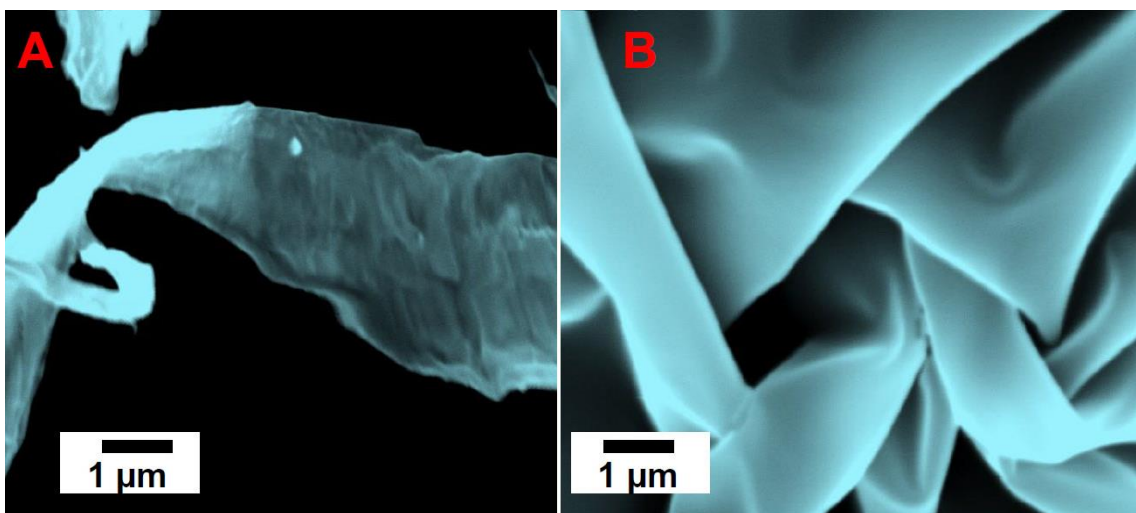
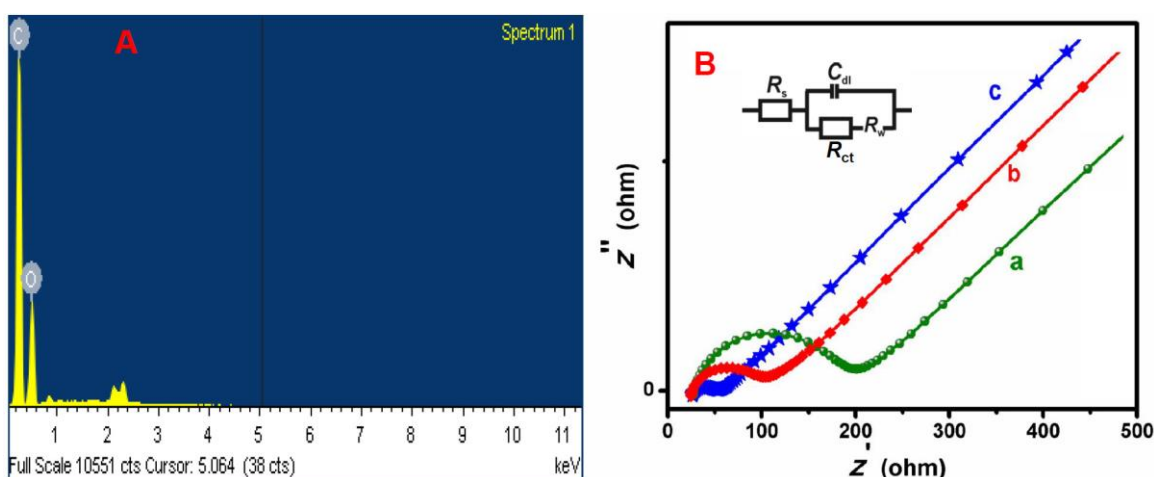**Figure 1.** SEM images of GONR (A and B)

Figure 2. (A) EDX spectrum of GONR. (B) EIS curves of unmodified SPCE (a) and GONR/SPCE (b) and MWCNTs/SPCE (c) in 0.1 M KCl containing 5 mM $Fe(CN)_6^{3-/4-}$. Amplitude: 5 mV, Frequency: 0.1 Hz to 100 kHz. Inset: Randles equivalent circuit model

3.2 Electrocatalysis of folic acid at GONR/SPCE

Figure 3 displays the cyclic voltammograms (CVs) obtained at unmodified SPCE (a), activated SPCE (b), MWCNTs/SPCE (c) and GONR/SPCE in phosphate buffer containing 2 μM FA. Compared with unmodified SPCE, activated SPCE has shown better electrocatalytic ability towards FA and hence we have adopted activated SPCE to fabricate modified electrodes in all our studies. Both MWCNTs and GONR have shown good electrocatalytic ability to FA. However, GONR/SPCE displays significantly enhanced catalytic peak current and less overpotential to oxidation of FA in comparison with MWCNTs/SPCE.
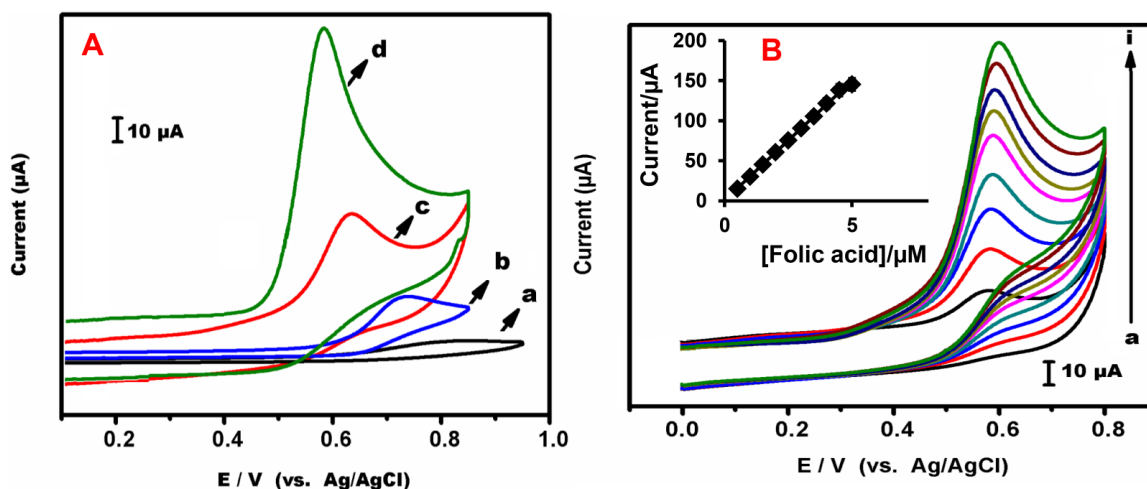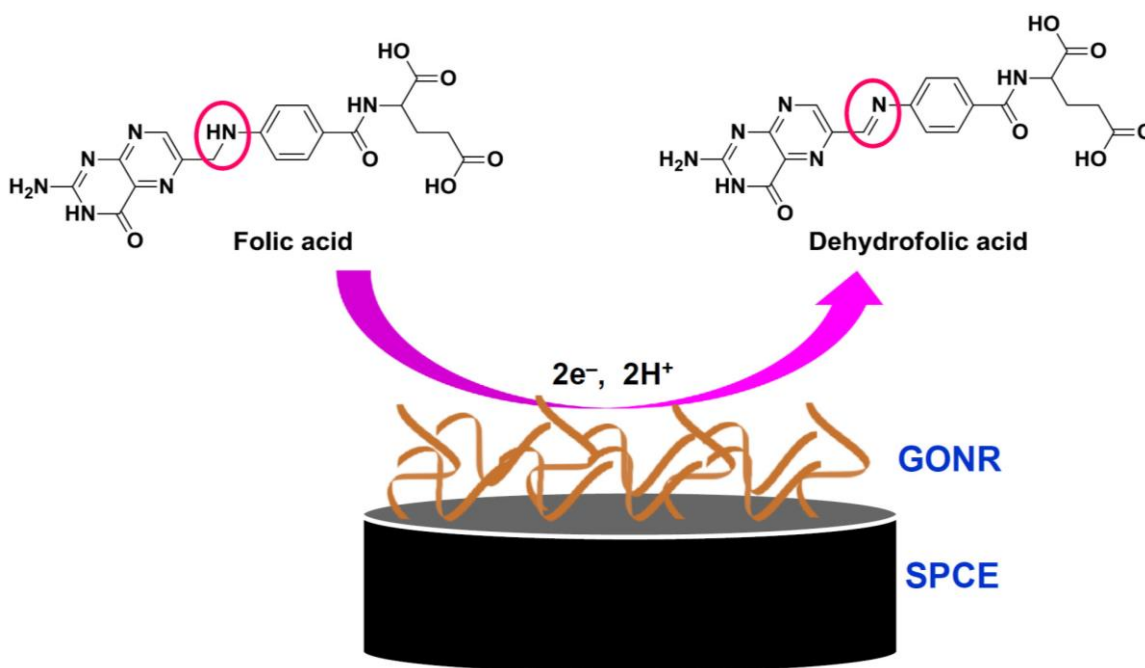
Figure 3. Cyclic voltammograms obtained at bare SPCE (a), activated SPCE (b), MWCNTs/SPCE (c) and GONR/SPCE (d) in phosphate buffer (pH 7.0) containing 2 μM folic acid. Scan rate= 50 mVs^{-1}. (B) Cyclic voltammograms obtained at GONR/SPCE towards different concentrations of FA (a to i; each 1 μM addition), Inset: current/μM vs. [Folic acid]/μA

Scheme 1. Electrochemical oxidation of folic acid at GONR/SPCE

The FA oxidation peak potential observed at GONR/SPCE is + 0.55 V, while its onset potential was observed at + 0.48 V. Thus, GONR/SPCE is shown superior electrocatalytic ability over MWCNTs with considerable shift in overpotential. The schematic representation for the oxidation of folic acid at GONR/SPCE is illustrated in **scheme 1** which is consistent with the previous reports [41]. The rich edge chemistry and abundant functional groups of GONR are highly responsible for the improved electrocatalysis [21, 22, 42-44]. Besides, GONR has large area-normalized edge-plane structures compared with GONR, and as a result the GONR/SPCE is better modified electrode than

MWCNTs/SPCE for electrochemical sensing of FA [45, 46]. Furthermore, the FA oxidation peak current increases linearly as the concentration of FA increases which indicate good electrocatalytic ability of the electrode without electrode fouling (Figure 3B). The plot between oxidation peak current and concentration of FA exhibits linear relationship (Inset to Fig. 3B). Next, the influence of scan rates to the oxidation of FA is investigated (Fig. 4A). The FA oxidation peak current linearly increases as the scan rate increases. The plot between peak current and square root of scan rates exhibits good linearity which indicating diffusion controlled process (Fig. 4B) [47].
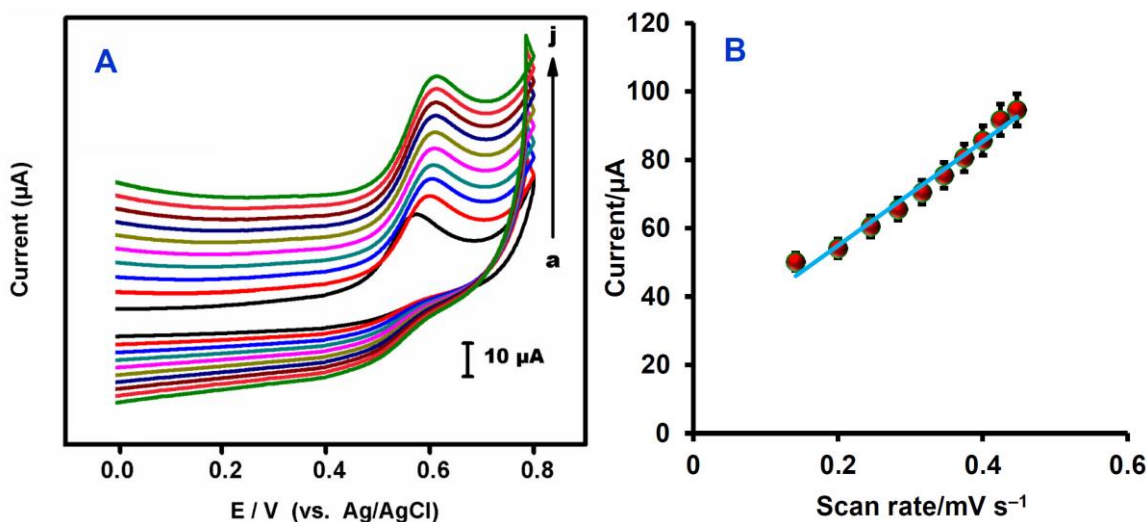

Figure 4. (A) Cyclic voltammograms of GONR/SPCE in phosphate buffer (pH 7) containing 2 µM folic acid at different scan rates (20 to 200 mV s^{-1}). B) Scan rate (mV s^{-1}) vs. peak currents (µA).
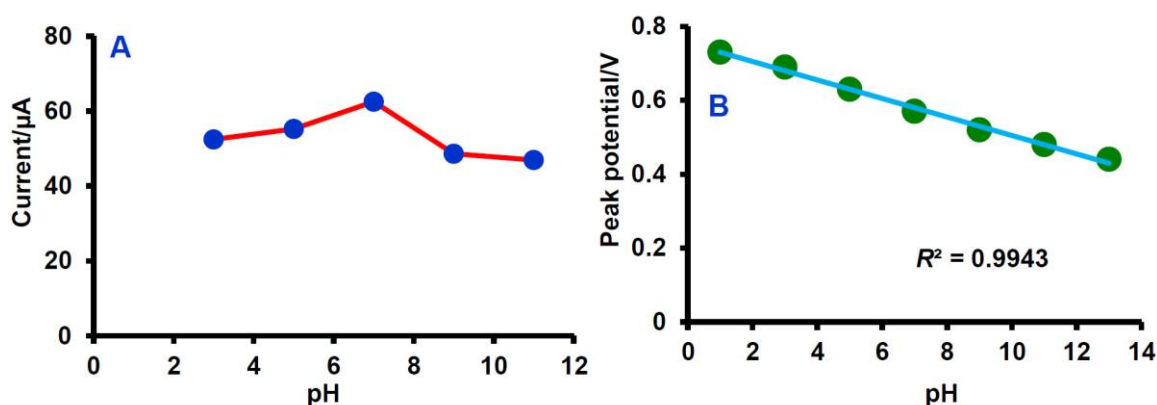

Figure 5. (A) Dependence of cathodic peak current with respect to pH. (B) Dependence of cathodic peak potential with pH

Next, the influence of buffer pH on the electrocatalytic oxidation of FA is investigated. As the pH of electrolyte changes, both peak current and peak potential of FA are changed accordingly. The peak current increases as the pH increases from 3.0 to 7.0 and reached maxima at pH 7.0 and the peak current decreases on further increase in pH 7.0 to 11.0 (Fig. 5A). Thus, the maximum electrocatalytic

ability is attained at neutral pH 7.0. The plot between different pH and peak potential displays good linearity (Fig. 5B) and this behaviour is consistent with the previous reports [1].

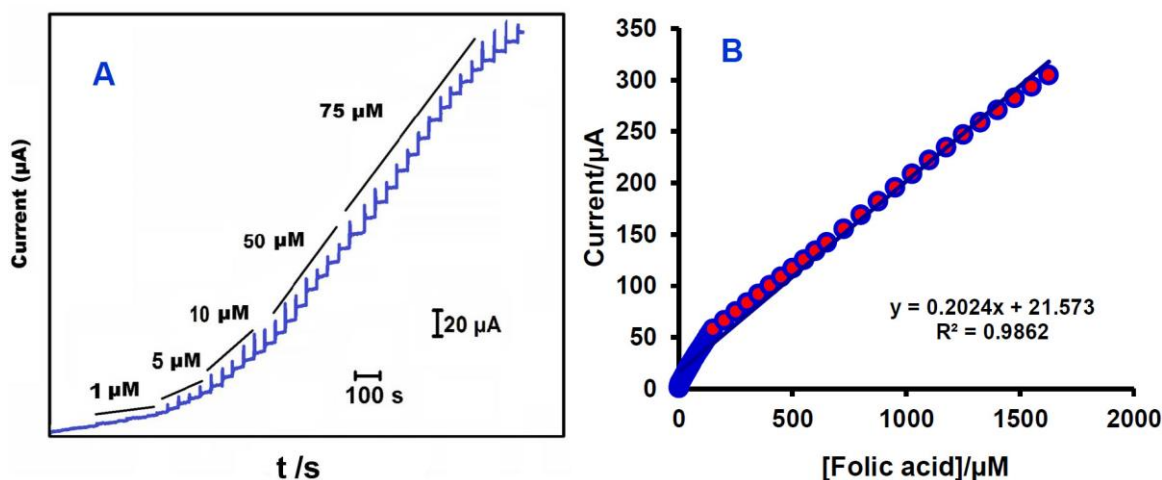### 3.3 Amperometric determination folic acid

Figure 6. (A) Amperometric response of GONR/SPCE upon each sequential additions FA into continuously stirred phosphate buffer (pH 7.0). $E_{app} = + 0.55$ V

Table 1. Comparison of analytical parameters for the determination of FA at GONR film modified electrode with reported works

Electrode	Linear range/μM	LOD/nM	Ref.
AuNPs modified gold electrode	0.01– 1	7.5	[48]
Ferrocenedicarboxylic acid/MWCNTs	4.6–152	1100	[49]
Porous silicon nanoparticles	1-1000	800	[50]
MoS$_2$/reduced graphene oxide	0.01–100	10	[11]
Hemoglobin/silica-coated magnetic nanoparticles	1–369	18	[51]
Graphene oxide nanoribbons	0.1–1600	20	This work

Fig. 6A displays the amperometric responses obtained at GONRs/SPCE for sequential additions of FA. The applied potential was + 0.55 V. For each addition, a sharp rise in amperometric current is observed and the response current reached 95% steady-state current within 5s of FA injection. Thus, the GONRs/SPCE electrode has rapid response time and this method can be used for rapid sensing of FA. The concentration dependent linear plot exhibits good linearity (Fig. 6B). The working concentration range was linear from 0.1–1600 μM with sensitivity of 0.675 μAμM^{-1} cm^{-2}. The limit of detection (LOD) was calculated as 20 nM. The LOD was calculated using the formula, LOD= 3 s_b/S where, s_b is the standard deviation of ten blank measurements and S is the sensitivity [17,

52]. The excellent analytical parameters such as wide linear range, high sensitivity and low detection limit achieved at GONRs/SPCE are revealing the potential of this method towards FA detection. The sensor parameters such as LOD, sensitivity and linear range of FA are compared with previously reported electrodes (Table 1). As seen from the table, the GONR film has either superior or competitive sensor performance over reported literature [11, 48–51]. Remarkably, we are using SPCE technology which is cheaper and highly reproducible and adding additional advantages to the developed method [53].

3.4 Stability, repeatability and reproducibility

In order to determine storage stability of the GONR/SPCE, its electrocatalytic response towards FA (100 nM) is monitored every day. During one week of storage period, the catalytic current slightly decreased, while 94.20% of the initial response current was retained which reveals good storage stability of the film which is consistent with our previous reports [54, 55]. In addition, the electrode exhibits appreciable repeatability with RSD of 3.84% for five repetitive measurements carried out using single electrode and it exhibits appreciable reproducibility with RSD of 3.42% for five independent measurements carried out in five different electrodes [56].

3.5 Real sample analysis

Practical applicability of the GONR/SPCE towards determination of FA is demonstrated in human urine sample. First human urine sample was diluted with phosphate buffer (pH 7) with 1:50 ratio. 0.2 µM and 0.4 µM of FA are spiked and used to perform amperometry experiment. The added, found and recovery values are presented in Table 2. The recovery values are in satisfactory range (97.16 to 98.55 %) which revealing potential practicality of the described method. Therefore, the developed method can be applicable for the real-time monition FA in real samples [57].

Table 2. Determination of FA in spiked human urine sample using GNS–MoS$_2$–AuNPs/SPCE

Urine sample	Added/µM	Found/µM	Recovery/%	RSD*/%
FA	0.2	0.195	97.5	3.56
	0.4	0.39	97.5	3.41

* Relative Standard Deviation (RSD) of three individual measurements

4. CONCLUSIONS

In summary, GONR has significantly enhanced electrocatalytic ability towards FA sensing in comparison with MWCNTs. Due to the presence of rich edge chemistry and abundant functional groups, and higher area-normalized edge-plane structures GONRs is surpassed the electrochemical

sensing ability of MWCNTs. The modified electrode has excellent sensor performance with wide linear range (0.1–1600 µM) and low detection limit (20 nM). The other advantages of the electrode are its reproducibility, repeatability, selectivity, stability and practical feasibility.

References

1. B. Unnikrishnan, Y.-L. Yang, S.-M. Chen, *Int. J. Electrochem. Sci.,* 6 (2011) 3224.
2. B.B. Prasad, R. Madhuri, M.P. Tiwari, P.S. Sharma, *Sens. Actuators B, Chemical,* 146 (2010) 321.
3. H. Yaghoubian, V. Nejad, S. Roodsaz, *Int. J. Electrochem. Sci.,* 5 (2010) 1411.
4. D. Zhang, X. Ouyang, W. Ma, L. Li, Y. Zhang, *Electroanalysis,* 28 (2016) 312.
5. P. Kalimuthu, S.A. John, *Biosens. Bioelectron.,* 24 (2009) 3575.
6. M.M. Foroughi, H. Beitollahi, S. Tajik, A. Akbari, R. Hosseinzadeh, *Int. J. Electrochem. Sci.,* 9 (2014) 8407.
7. A.R. Taheri, A. Mohadesi, D. Afzali, H. Karimi-Maleh, *Int. J. Electrochem. Sci.,* 6 (2011) 171.
8. R. Shashanka, D. Chaira, B.K. Swamy, *Int. J. Electrochem. Sci.,* 10 (2015) 5586.
9. T.S.K. Naik, B.K. Swamy, C. Vishwanath, M. Kumar, *J. Anal. Bioanal. Tech.,* 6 (2015) 1000272.
10. K. Cinková, Ľ. Švorc, P. Šatkovská, M. Vojs, P. Michniak, M. Marton, *Anal. Lett.,* 49 (2016) 107.
11. F. Chekin, F. Teodorescu, Y. Coffinier, G.-H. Pan, A. Barras, R. Boukherroub, S. Szunerits, *Biosens. Bioelectron.,* 85 (2016) 807.
12. M. Mazloum-Ardakani, M.A. Sheikh-Mohseni, M. Abdollahi-Alibeik, A. Benvidi, Sens. Actuators, B, 171 (2012) 380.
13. L. Mirmoghtadaie, N. Shamaeizadeh, N. Mirzanasiri, *Int. J. preventive Med.,* 6 (2015) 100.
14. B. Dinesh, V. Mani, R. Saraswathi, S.-M. Chen, *RSC Adv.,* 4 (2014) 28229.
15. B. Devadas, V. Mani, S.-M. Chen, *Int. J. Electrochem. Sci.,* 7 (2012) 8064.
16. V. Mani, A.E. Vilian, S.-M. Chen, *Int. J. Electrochem. Sci,* 7 (2012) 12774.
17. V. Mani, A.P. Periasamy, S.-M. Chen, *Electrochem. Commun.,* 17 (2012) 75.
18. R. Devasenathipathy, V. Mani, S.-M. Chen, K. Manibalan, S.-T. Huang, *Int. J. Electrochem. Sci,* 10 (2015) 1384.
19. X. Li, X. Wang, L. Zhang, S. Lee, H. Dai, *Science*, 319 (2008) 1229.
20. M. Sprinkle, M. Ruan, Y. Hu, J. Hankinson, M. Rubio-Roy, B. Zhang, X. Wu, C. Berger, W.A. De Heer, *Nat. Nanotechnol.,* 5 (2010) 727.
21. X. Lu, H.M. Chan, C.-L. Sun, C.-M. Tseng, C. Zhao, *J. Mater. Chem, A,* 3 (2015) 13371.
22. A.L. Higginbotham, D.V. Kosynkin, A. Sinitskii, Z. Sun, J.M. Tour, *ACS nano,* 4 (2010) 2059.
23. D.V. Kosynkin, A.L. Higginbotham, A. Sinitskii, J.R. Lomeda, A. Dimiev, B.K. Price, J.M. Tour, *Nature,* 458 (2009) 872.
24. A. Zehtab Yazdi, K. Chizari, A.S. Jalilov, J. Tour, U. Sundararaj, *ACS nano*, 9 (2015) 5833.
25. Y. Gong, H. Fei, X. Zou, W. Zhou, S. Yang, G. Ye, Z. Liu, Z. Peng, J. Lou, R. Vajtai, *Chem. Mater.,* 27 (2015) 1181.
26. A. Martín, P. Batalla, J. Hernández-Ferrer, M.T. Martínez, A. Escarpa, *Biosens. Bioelectron.,* 68 (2015) 163.
27. L. Shang, F. Zhao, B. Zeng, *Electrochim. Acta,* 168 (2015) 330.
28. Y. Yi, G. Zhu, X. Wu, K. Wang, *Biosens. Bioelectron.,* 77 (2016) 353.
29. W.-J. Guan, Y. Li, Y.-Q. Chen, X.-B. Zhang, G.-Q. Hu, *Biosens. Bioelectron.,* 21 (2005) 508.
30. M. Bilgi, E. Ayranci, *Sens. Actuators, B,* 237 (2016) 849.

31. M. Thiruppathi, N. Thiyagarajan, M. Gopinathan, J.-M. Zen, *Electrochem. Commun.,* 69 (2016) 15.
32. N. Thiyagarajan, J.-L. Chang, K. Senthilkumar, J.-M. Zen, *Electrochem. Commun.,* 38 (2014) 86.
33. L.-Y. Lin, M.-H. Yeh, J.-T. Tsai, Y.-H. Huang, C.-L. Sun, K.-C. Ho, *J. Mater. Chem. A,* 1 (2013) 11237-11245.
34. A. Martín, J. Hernández-Ferrer, M.T. Martínez, A. Escarpa, *Electrochim. Acta,* 172 (2015) 2.
35. C.H.A. Wong, C.K. Chua, B. Khezri, R.D. Webster, M. Pumera, *Angew. Chem. Int. Ed.,* 125 (2013) 8847.
36. A.J. Bard, L.R. Faulkner, Electrochemical methods: fundamentals and applications, Wiley New York1980.
37. V.F. Lvovich, Impedance spectroscopy: applications to electrochemical and dielectric phenomena, John Wiley & Sons 2012.
38. V. Mani, R. Devasenathipathy, S.-M. Chen, S.-T. Huang, V. Vasantha, *Enzyme Microb. Technol.,* 66 (2014) 60.
39. M.E. Orazem, B. Tribollet, Electrochemical impedance spectroscopy, John Wiley & Sons 2011.
40. T.-C. Lin, Y.-S. Li, W.-H. Chiang, Z. Pei, *Biosens. Bioelectron.,* (2016), DOI http://dx.doi.org/10.1016/j.bios.2016.03.046i
41. T. Maiyalagan, J. Sundaramurthy, P.S. Kumar, P. Kannan, M. Opallo, S. Ramakrishna, *Analyst*, 138 (2013) 1779.
42. L. Shi, X. Niu, T. Liu, H. Zhao, M. Lan, *Microchim. Acta,* 182 (2015) 2485.
43. Z.-L. Wu, C.-K. Li, J.-G. Yu, X.-Q. Chen, *Sens. Actuators, B,* 239 (2017) 544.
44. E. Mehmeti, D.M. Stanković, A. Hajrizi, K. Kalcher, *Talanta,* 159 (2016) 34.
45. J. Qian, X. Yang, Z. Yang, G. Zhu, H. Mao, K. Wang, *J. Mater. Chem. B,* 3 (2015) 1624.
46. Y. Pan, L. Shang, F. Zhao, B. Zeng, *Electrochim. Acta*, 151 (2015) 423.
47. N. Boes, H. Züchner, J. Less-Common Met. 49 (1976) 223.
48. L. Mirmoghtadaie, A.A. Ensafi, M. Kadivar, M. Shahedi, M.R. Ganjali, *Int. J. Electrochem. Sci,* 8 (2013) 3755.
49. A.A. Ensafi, H. Karimi-Maleh, *J. Electroanal. Chem.,* 640 (2010) 75.
50. T. Nie, L. Lu, L. Bai, J. Xu, K. Zhang, O. Zhang, Y. Wen, L. Wu, *Int. J. Electrochem. Sci.,* 8 (2013) 7016-7029.
51. J. Ghodsi, A. Hajian, A.A. Rafati, Y. Shoja, O. Yurchenko, G. Urban, J. Electrochem. Soc., 163 (2016) B609.
52. M. Govindasamy, S.-M. Chen, V. Mani, R. Devasenathipathy, R. Umamaheswari, K.J. Santhanaraj, A. Sathiyan, *J. colloid interface Sci.,* 485 (2017) 129.
53. S.A. Wring, J.P. Hart, *Analyst,* 117 (1992) 1281.
54. M. Govindasamy, V. Mani, S.-M. Chen, A. Sathiyan, J.P. Merlin, V.K. Ponnusamy, *Int. J. Electrochem. Sci.,* 11 (2016) 8730.
55. M. Govindasamy, V. Mani, S.-M. Chen, R. Karthik, K. Manibalan, R. Umamaheswari, *Int. J. Electrochem. Sci.,* 11 (2016) 2954.
56. M. Govindasamy, S.-M. Chen, V. Mani, A. Sathiyan, J.P. Merlin, F.M. Al-Hemaid, M.A. Ali, *RSC Adv.,* 6 (2016) 100605.
57. S. Akbar, A. Anwar, Q. Kanwal, *Anal. Biochem.,* 510 (2016) 98.